Synthesis of Organoboron Quinoline-8-thiolate and Quinoline-8-selenolate Complexes and Their Incorporation into the π-Conjugated Polymer Main-Chain

Yuichiro Tokoro, Atsushi Nagai, Kenta Kokado, and Yoshiki Chujo*

Department of Polymer Chemistry, Graduate School of Engineering, Kyoto University, Katsura, Nishikyo-ku, Kyoto 615-8510, Japan

Received January 5, 2009; Revised Manuscript Received February 22, 2009

ABSTRACT: Low-molecular-mass organoboron quinoline-8-thiolate and -selenolate complexes as model compounds, and organoboron polymers incorporated their complex structures into the poly(*p*-phenylene-ethynylene) main chain were prepared. Tetracoordination states of boron atoms in the obtained compounds were confirmed by ^{11}B NMR spectroscopy, and the detailed structures of the model compounds were determined by single-crystal X-ray diffraction analysis. The polymers were synthesized by Sonogashira-Hagihara coupling reaction of organoboron quinolate-based monomers having diiodo groups with 1,4-diethynylbenzene derivatives bearing electron-donating or -withdrawing groups in moderate yields. Their optical properties were studied by UV−vis absorption and photoluminescence spectroscopies. Increasing atomic number of the 16 Group atom adjacent to the boron atom caused emission shift to longer wavelength and decreasing of absolute quantum yields for both the model compounds and the polymers. There are no differences between the polymers with the donating π-conjugated linker and with the accepting one in the photoluminescence property, resulting from efficient energy transfer from π-conjugated main chain to Q ligand. Furthermore, the obtained polymers showed high refractive indices (n_d > 1.66).

Introduction

In recent years, there has been a considerable interest in conjugated polymers due to their potential use in a wide range of applications in electronics and photonics favored by their tunable electronic and optical properties.[1,2] Their prime examples are polymeric light emitting diodes,[2] plastic lasers,[3] nonlinear optical materials,[4] and polymer-based photovoltaic cells.[5] In addition, other advantages of organic conjugated polymers over their inorganic counterparts are the application of device fabrication via solution processing methods including dip coating, spin casting, and, ink-jet printing which receive more and more attention as a potential low cost alternative to vacuum deposition techniques.[6]

More recently, an incorporation of organoboron dyes as electroluminescent chromophores into π-conjugated polymer main chain, i.e., π-conjugated organoboron polymer, is attractive for future applications as electroluminescent devices, organic field-effect transistors, photovoltaics, and so on. Organoboron dyes are well-known in the fields of molecular probes,[7] photosensitizers,[8] and lasers[9] because their dyes possess large molar coefficients, two-photon absorption cross sections, high emission quantum yields and sensitivity to the surrounding medium. Conjugated polymers containing organoboron quinolate, which is one of the organoboron dyes, in their main chain have been synthesized in our group.[10] These polymers showed strong green fluorescence and an efficient energy migration from conjugated linkers to boron quinolate moieties was observed.

Quinolate-type ligands (Q), such as 8-hydroxyquinoline and quinoline-8-thiol, have been widely used to produce luminescent metal complexes, which in many cases emit from a Q-based intraligand charge transfer (ILCT) excited state.[11] This ILCT state is formed when the highest occupied molecular orbital (HOMO) and the lowest unoccupied molecular orbital (LUMO) are localized on the phenolate/thiolate ring and on the pyridyl ring of the Q ligand, respectively. A few general rules which govern the fluorescence of metal chelates of 8-hydroxyquinoline have been formulated.[12] (i) Fluorescence is reduced with increasing atomic number of the metal ion, caused by an increase in the rate of intersystem crossing known as heavy atom effect. For example, tris(8-hydroxyquinolinato)indium is less fluorescent compared to tris(8-hydroxyquinolinato)gallium which, in turn, is less fluorescent than tris(8-hydroxyquinolinato)aluminum (AlQ_3). (ii) The emission shifts to longer wavelength as the covalent nature of the metal−ligand bonding is increased. For example, the chelates formed with Al, Ga, and In emit at progressively longer wavelengths of 532, 545, 558 nm, respectively. Likewise, metal chelates of 8-hydroxyquinoline and quinoline-8-thiol absorb and emit at increasingly longer wavelengths.[13] In contrast, the application of these rules to organoboron quinolate has not yet been investigated. Herein, we report the synthesis and optical properties of the low-molecular-mass organoboron quinoline-8-thiolate and -selenolate complexes and incorporation of the organoboron quinoline-8-thiolate or -selenolate into the conjugated polymer main chain.

Experimental Section

Measurements. ^{1}H (400 MHz), ^{13}C (100 MHz), and ^{11}B (128 MHz) NMR spectra were recorded on a JEOL JNM-EX400 spectrometer. ^{1}H and ^{13}C NMR spectra used tetramethylsilane (TMS) as an internal standard, ^{11}B NMR were referenced externally to BF_3OEt_2 (sealed capillary) in $CDCl_3$. The number-average molecular weight (M_n) and the molecular weight distribution [weight-average molecular weight/number-average molecular weight (M_w/M_n)] values of all polymers were estimated by size-exclusion chromatography (SEC) with a TOSOH G3000HXI system equipped with three consecutive polystyrene gel columns [TOSOH gels: α-4000, α-3000, and α-2500] and ultraviolet detector at 40 °C. The system was operated at a flow rate of 1.0 mL/min, with tetrahydrofuran as an eluent. Polystyrene standards were employed for calibration. UV−vis spectra were recorded on a Shimadzu UV-3600 spectrophotometer. Fluorescence emission spectra were recorded on a HORIBA JOBIN YVON Fluoromax-4 spectrofluorometer, and the absolute quantum yield was calculated by integrating sphere method on the HORIBA JOBIN YVON Fluo-

* Corresponding author. E-mail: chujo@chujo.synchem.kyoto-u.ac.jp.

10.1021/ma900008m CCC: $40.75
Published on Web 03/20/2009

romax-4 spectrofluorometer in chloroform. FT-IR spectra were obtained using a Perkin-Elmer 1600 infrared spectrometer. Thermogravimetric analyses (TGA) were performed on a Seiko TG/DTA 6200 at a scan rate of 10 °C/min. X-ray crystallographic analysis was carried out by a Rigaku R-AXIS RAPID-F graphite-monochromated Mo Kα radiation diffractometer with an imaging plate. A symmetry related absorption correction was carried out by using the program ABSCOR.[14] The analysis was carried out with direct methods (SHELX-97[15] or SIR97[16]) using Yadokari-XG.[17] The program ORTEP3[18] was used to generate the X-ray structural diagram. Elemental analysis was performed at the Microanalytical Center of Kyoto University. Refractive indices were measured by an ATAGO Abbe refractometer DR-M4.

Materials. Tetrahydrofuran (THF) and triethylamine (Et_3N) were purified using a two-column solid-state purification system (Glass-contour System, Joerg Meyer, Irvine, CA). B(4-iodophenyl)$_2$Q (**2O**),[10] quinoline-8-selenol,[19] 1,4-diethynyl-2,5-dihexadecyloxybenzene,[20] and 1,4-diethynyl-2,5-bis(trifluoromethyl)benzene[21] were prepared according to the literature.

Synthesis of BPh2Q (1O). Triphenylborane (0.484 g, 2.00 mmol) dissolved in toluene (8 mL) was added to a solution of 8-hydroxyquinoline (0.292 g, 2.01 mmol) stirring in toluene (16 mL). After the reaction mixture was refluxed for 11.5 h, the solvent was removed under vacuum. The crude product was put in a small vial and then dissolved in CH_2Cl_2, on which hexane was slowly laid. The phase separated solution was allowed to stand for 25 h for slow evaporation and diffusion, which gave a yellow solid of **1O** (0.369 g, 1.19 mmol) in 59% yield. ^{1}H NMR ($CDCl_3$, δ, ppm): 8.58 (d, J = 5.16 Hz, 1H), 8.40 (d, J = 8.28 Hz, 1H), 7.68−7.60 (m, 2H), 7.45 (d, J = 6.56 Hz, 2H), 7.29−7.21 (m, 7H), 7.18 (d, J = 7.80 Hz, 1H).

Synthesis of BPh2Q−S (1S). Triphenylborane (1.070 g, 4.40 mmol) dissolved in toluene (16 mL) was added to a solution of 8-mercaptoquinoline hydrochloride (0.791 g, 4.00 mmol) and Et_3N (0.56 mL, 4.00 mmol) stirring in toluene (16 mL). After the reaction mixture was refluxed for 12 h, the solvent was removed under vacuum. The remaining solid was dissolved in $CHCl_3$, followed by washing with water, drying over $MgSO_4$, and removal of the solvent under vacuum. The crude product was put in a small vial and then dissolved in CH_2Cl_2, on which hexane was slowly laid. The phase separated solution was allowed to stand for 25 h for slow evaporation and diffusion, which gave a yellow solid of **1S** (0.380 g, 1.17 mmol) in 29% yield. ^{1}H NMR ($CDCl_3$, δ, ppm): 8.50 (d, J = 5.36 Hz, 1H), 8.46 (d, J = 7.32 Hz, 1H), 7.73 (d, J = 7.32 Hz, 1H), 7.62−7.56 (m, 2H), 7.49 (d, J = 8.08 Hz, 1H), 7.33 (d, J = 6.84 Hz, 4H), 7.28−7.18 (m, 6H). ^{13}C NMR ($CDCl_3$, δ, ppm): 144.58, 144.16, 143.34, 141.04, 133.20, 130.95, 129.35, 127.55, 127.00, 126.47, 121.59, 118.70. ^{11}B NMR ($CDCl_3$, δ, ppm): 3.57. HRMS (EI): calcd for $C_{21}H_{16}NSB$, m/z 325.1097; found, m/z 325.1100.

Synthesis of BPh2Q−Se (1Se). Triphenylborane (0.434 g, 1.79 mmol) dissolved in toluene (7.2 mL) was added to a solution of quinoline-8-selenol (0.373 g, 1.79 mmol) stirring in toluene (16 mL). After the reaction mixture was refluxed for 12 h, the solvent was slowly evaporated for recrystallization, giving a yellow solid of **1Se** (0.327 g, 0.878 mmol) in 49% yield. ^{1}H NMR ($CDCl_3$, δ, ppm): 8.49 (m, 2H), 7.97 (d, J = 7.32 Hz, 1H), 7.64−7.52 (m, 3H), 7.33 (d, J = 6.80 Hz, 4H), 7.26−7.17 (m, 6H). ^{13}CNMR ($CDCl_3$, δ, ppm): 145.88, 144.63, 141.70, 138.74, 133.54, 131.56, 130.85, 129.94, 127.54, 126.38, 121.40, 120.61. ^{11}B NMR ($CDCl_3$, δ, ppm): 3.66. HRMS (EI): calcd for $C_{21}H_{16}NBSe$, m/z 373.0541; found, m/z 373.0537.

Synthesis of B(4-iodophenyl)$_2$Q−S (2S). A 12.5 mL (1.6 M, 20 mmol) aliquot of n-BuLi was slowly added to a solution of 1,4-diiodobenzene (6.60 g, 20 mmol) in 100 mL of THF at −78 °C, and the mixture was stirred at −78 °C for 1 h. BBr_3 (0.67 mL, 6.7 mmol) was added to the reaction mixture at −78 °C and then allowed to room temperature and refluxed for 3.5 h. The mixture of 8-mercaptoquinoline hydrochloride (1.38 g, 7.0 mmol) and Et_3N (0.98 mL, 7.0 mmol) dissolved in 60 mL of THF in another flask was added to the reaction mixture and then refluxed for 9 h. The solvents were removed under vacuum. The residue was dissolved in a small amount of $CHCl_3$ and reprecipitating with 100 mL of methanol, giving a yellow solid. This solid was purified by dissolving in a small amount of CH_2Cl_2 and reprecipitating with 80 mL of hexane to obtain **2S** (1.92 g, 3.3 mmol) in 50% yield as a yellow solid. ^{1}H NMR ($CDCl_3$, δ, ppm): 8.51 (d, J = 8.32 Hz, 1H), 8.43 (d, J = 4.12 Hz, 1H), 7.74 (d, J = 7.32 Hz, 1H), 7.66−7.53 (m, 7H), 7.03 (d, J = 8.04 Hz, 4H). ^{13}CNMR ($CDCl_3$, δ, ppm): 143.91, 141.53, 136.67, 135.16, 131.20, 129.40, 127.30, 121.73, 119.10, 93.12. ^{11}B NMR ($CDCl_3$, δ, ppm): 7.43. HRMS (EI): calcd for $C_{21}H_{14}NSBI_2$, m/z 576.9029; found, m/z 576.9029. Anal. Calcd for $C_{21}H_{14}NSBI_2$: C, 43.71; H, 2.45; I, 43.99. Found: C, 43.69; H, 2.63; I, 43.79.

Synthesis of B(4-iodophenyl)$_2$Q−Se (2Se). A 7.1 mL (1.6 M, 11 mmol) aliquot of n-BuLi was slowly added to the solution of 1,4-diiodobenzene (3.73 g, 11 mmol) in 57 mL of THF at −78 °C, and the mixture was stirred at −78 °C for 1 h. BBr_3 (0.36 mL, 3.8 mmol) was added to the reaction mixture at −78 °C and then allowed to room temperature and refluxed for 1 h. Quinoline-8-selenol (0.78 g, 3.8 mmol) dissolved in 50 mL of THF in another flask was added to the reaction mixture and then refluxed for 12 h. The solvents were removed under vacuum. The residue was dissolved in a small amount of $CHCl_3$ and reprecipitating with 50 mL of methanol, giving an orange solid. This solid was purified by dissolving in a small amount of CH_2Cl_2 and reprecipitating with 30 mL of hexane to obtain **2Se** (0.45 g, 0.72 mmol) in 19% yield as an orange solid. ^{1}H NMR ($CDCl_3$, δ, ppm): 8.54 (d, J = 8.28 Hz, 1H), 8.41 (d, J = 5.40 Hz, 1H), 7.98 (d, J = 7.32 Hz, 1H), 7.68−7.55 (m, 7H), 7.03 (d, J = 8.28 Hz, 4H). ^{13}C NMR ($CDCl_3$, δ, ppm): 145.59, 144.51, 142.16, 137.99, 136.65, 135.46, 131.79, 131.09, 129.99, 121.54, 120.96, 100.55, 92.95. ^{11}B NMR ($CDCl_3$, δ, ppm): 7.53. HRMS (EI): calcd for $C_{21}H_{14}NBSeI_2$, m/z 624.8474; found, m/z 624.8472. Anal. Calcd for $C_{21}H_{14}NBSeI_2$: C, 40.43; H, 2.26; I, 40.68. Found: C, 40.68; H, 2.46; I, 40.53.

Synthesis of Polymer 4SO. Monomer **2S** (0.127 g, 0.220 mmol), 1,4-diethynyl-2,5-dihexadecyloxybenzene (0.134 g, 0.220 mmol), CuI (0.006 g, 0.030 mmol), and $Pd(PPh_3)_4$ (0.013 g, 0.011 mmol) were dissolved in 4.4 mL of THF and 2.2 mL of Et_3N. The reaction mixture was stirred at room temperature for 96 h. The solvent was removed under vacuum. The residue was purified by repeated precipitation from a small amount of $CHCl_3$ into 25 mL of methanol to obtain **4SO** (0.169 g, 0.183 mmol) in 83% yield as a yellow solid. ^{1}H NMR ($CDCl_3$, δ, ppm): 8,50 (2H), 7.77−7.52 (5H), 7.42 (4H), 7.29 (4H), 6.96 (2H), 3.99 (4H), 1.80 (4H), 1.49 (4H), 1.23 (48H), 0.85 (6H). ^{13}C NMR ($CDCl_3$, δ, ppm): 153.58, 144.23, 144.08, 143.33, 133.04, 131.08, 130.76, 129.43, 127.21, 121.71, 121.51, 118.95, 117.06, 114.08, 95.46, 85.53, 69.63, 31.93, 29.67, 29.37, 28.89, 25.98, 22.70, 14.11. ^{11}B NMR ($CDCl_3$, δ, ppm): 6.45. IR (KBr, ν, cm^{-1}): 3063, 3016, 2923, 2852, 2205, 1598, 1573, 1499, 1463, 1414, 1373, 1307, 1279, 1217, 1020, 865, 809, 776, 719.

Synthesis of Polymer 4SeO. Similar to the preparation of **4SO**, polymer **4SeO** was prepared from monomer **2Se** (0.137 g, 0.220 mmol) and 1,4-diethynyl-2,5-dihexadecyloxybenzene (0.134 g, 0.220 mmol) in 87% yield as an orange solid. ^{1}H NMR ($CDCl_3$, δ, ppm): 8,54 (1H), 8.46 (1H), 7.99 (1H), 7.66−7.55 (4H), 7.41 (4H), 7.28 (4H), 3.98 (4H), 1.80 (4H), 1.23 (48H), 0.87 (6H). ^{11}B NMR ($CDCl_3$, δ, ppm): 5.18. IR (KBr, ν, cm^{-1}): 3063, 3014, 2921, 2851, 2204, 1597, 1571, 1495, 1466, 1412, 1377, 1304, 1279, 1216, 1008, 862, 818, 754.

Synthesis of Polymer 4SF. Similar to the preparation of **4SO**, polymer **4SF** was prepared from monomer **2S** (0.144 g, 0.250 mmol) and 1,4-diethynyl-2,5-bis(trifluoromethyl)benzene (0.066 g, 0.25 mmol), in 58% yield as a yellow solid. ^{1}H NMR ($CDCl_3$, δ, ppm): 8,55−8.47 (2H), 7.90 (2H), 7.77 (1H), 7.65−7.55 (4H), 7.45 (4H), 7.33 (4H). ^{11}B NMR ($CDCl_3$, δ, ppm): 3.91. IR (KBr, ν, cm^{-1}): 3069, 2214, 1605, 1574, 1500, 1462, 1422, 1372, 1304, 1245, 1222, 1156, 1071, 1019, 913, 871, 820, 762.

Synthesis of Polymer 4SeF. Similar to the preparation of **4SO**, polymer **4SeF** was prepared from monomer **2Se** (0.156 g, 0.250 mmol) and 1,4-diethynyl-2,5-bis(trifluoromethyl)benzene (0.066 g, 0.25 mmol) in 69% yield as an orange solid. ^{1}H NMR ($CDCl_3$, δ, ppm): 8,57 (1H), 8.47 (1H), 8.00 (1H), 7.90 (2H), 7.70 (2H), 7.46 (9H), 7.29 (2H), 7.23 (1H). ^{11}B NMR ($CDCl_3$, δ, ppm): 4.89. IR

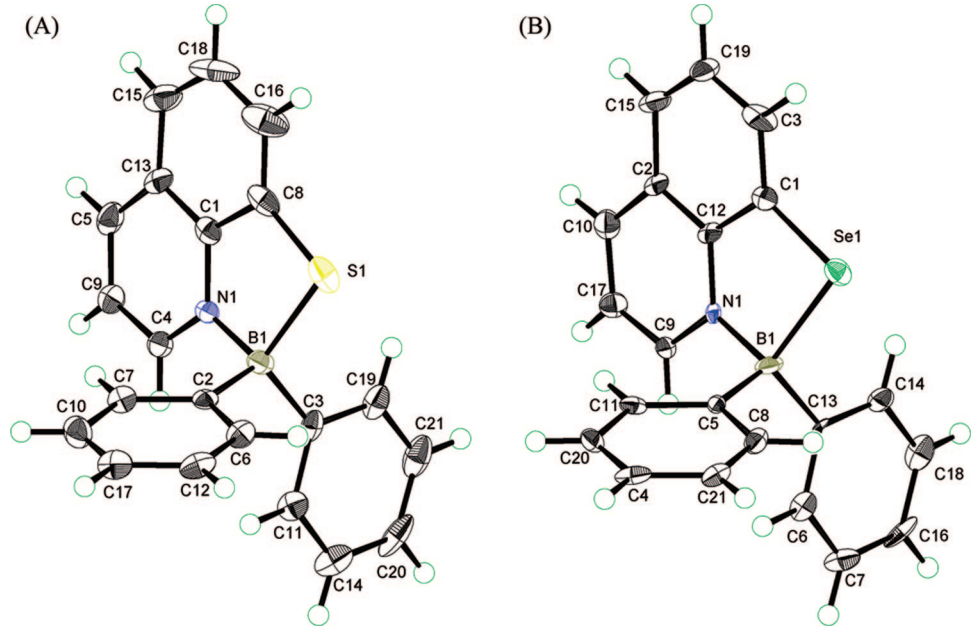

Figure 1. X-ray crystal structures of (A) **1S** and (B) **1Se** with thermal ellipsoids drawn to the 50% probability level.

(KBr, ν, cm^{-1}): 3065, 3015, 2212, 1601, 1573, 1497, 1459, 1422, 1372, 1303, 1245, 1221, 1157, 1071, 1011, 913, 870, 819, 754.

Synthesis of Polymer 4OO. Similar to the preparation of **4SO**, polymer **4OO** was prepared from monomer **2O** (0.134 g, 0.220 mmol) and 1,4-diethynyl-2,5-dihexadecyloxybenzene (0.134 g, 0.220 mmol) at 40 °C for 48 h in 29% yield as a yellow solid. ^{1}H NMR ($CDCl_3$, δ, ppm): 8,56 (1H), 8.44 (1H), 8.00 (1H), 7.67−7.54 (2H), 7.42 (7H), 7.26−7.19 (2H), 6.96 (2H), 3.98 (4H), 1.80 (4H), 1.49 (4H), 1.22 (48H), 0.86 (6H). ^{11}B NMR ($CDCl_3$, δ, ppm): 8.89. IR (KBr, ν, cm^{-1}): 3064, 3023, 2924, 2852, 2206, 1615, 1505, 1468, 1414, 1383, 1332, 1274, 1215, 1124, 1019, 957, 906, 865, 815, 783, 720.

Synthesis of Polymer 4OF. Similar to the preparation of **4SO**, polymer **4OF** was prepared from monomer **2O** (0.140 g, 0.250 mmol) and 1,4-diethynyl-2,5-bis(trifluoromethyl)benzene (0.066 g, 0.25 mmol) in 58% yield as a yellow solid. ^{1}H NMR ($CDCl_3$, δ, ppm): 8,56 (1H), 8.46 (1H), 8.00 (1H), 7.90 (2H), 7.70−7.56 (4H), 7.44 (4H), 7.33 (4H). ^{11}B NMR ($CDCl_3$, δ, ppm): 4.89. IR (KBr, ν, cm^{-1}): 3065, 3015, 2212, 1601, 1573, 1497, 1459, 1422, 1372, 1303, 1245, 1221, 1157, 1071, 1011, 913, 870, 819, 754.

Results and Discussion

Synthesis of Model Compounds. The reaction between 8-hydroxyquinoline, 8-mercaptoquinoline hydrochloride, or quinoline-8-selenolate and triphenylborane afforded the corresponding organoboron quinolates **1O**,[22] **1S**, and **1Se**, respectively. When these compounds were purified by recrystallization in the mixed solvent (CH_2Cl_2/hexane = 1/2 (v/v)), **1O**, **1S**, and **1Se** were obtained as yellow-green, yellow, and orange colored solids, respectively. All three compounds were stable under air and showed high solubillity in dichloromethane and chloroform. The tetracoordination state of the boron atoms in **1S** and **1Se** were confirmed by the ^{11}B NMR spectroscopy in $CDCl_3$ [**1S**, δ_B = 3.57 ppm; **1Se**, δ_B = 3.66 ppm], and the basic structures of **1S** and **1Se** were also characterized by ^{1}H NMR, ^{13}C NMR and EI mass spectroscopies.

Furthermore, the molecular structures of **1S** and **1Se** as determined by single crystal X-ray analyses are shown in Figure 1. The sp^3 orbital-hybridized boron centers of **1S** and **1Se** appear as a distorted tetrahedron with dihedral angles N(1)−B(1)−S(1) of 99.1 ° and N(1)−B(1)−Se(1) of 98.9 °, respectively (Table 1). The average of B(1)−N(1) bond length of **1Se** (1.608 Å) was slightly longer than that of **1S** (1.594 Å), probably indicating that the chelating ability of **1Se** is lower than that of **1S** because selenium atom brings about the larger distortion of five-membered chelating ring.

Table 1. Selected Bond Lengths (Å) and Angles (deg) for 1S and 1Se

		1S	
B(1)−N(1)	1.594(5)	N(1)−B(1)−S(1)	99.1(2)
B(1)−S(1)	1.980(4)	B(1)−S(1)−C(8)	93.09(18)
S(1)−C(8)	1.754(4)	S(1)−C(8)−C(1)	113.3(3)
C(8)−C(1)	1.418(5)	C(8)−C(1)−N(1)	115.7(3)
N(1)−C(1)	1.366(4)	C(1)−N(1)−B(1)	117.1(3)
B(1)−C(2)	1.608(6)		
B(1)−C(3)	1.602(6)		
		1Se	
B(1)−N(1)	1.608(8)	N(1)−B(1)−Se(1)	98.9(4)
B(1)−Se(1)	2.119(6)	B(1)−Se(1)−C(1)	88.8(2)
Se(1)−C(1)	1.887(6)	Se(1)−C(1)−C(12)	113.5(5)
C(1)−C(12)	1.429(6)	C(1)−C(12)−N(1)	117.1(6)
N(1)−C(12)	1.358(7)	C(12)−N(1)−B(1)	119.4(4)
B(1)−C(5)	1.599(7)		
B(1)−C(13)	1.604(8)		

Scheme 1. Synthesis of Model Compounds (A) 1O and 1Se and (B) 1S

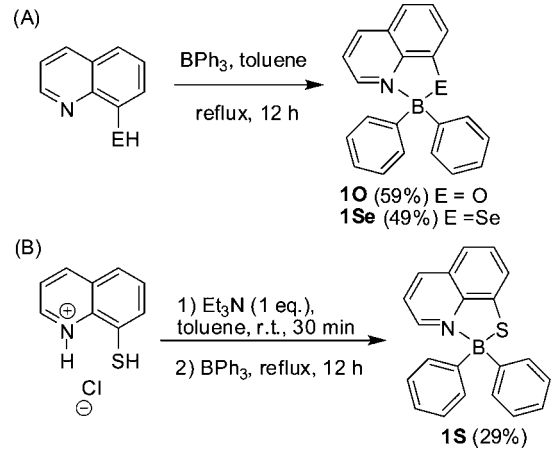

Synthesis of Monomers. Organoboron quinolate-based monomers **2O**,[10] **2S**, and **2Se** were prepared from the corresponding quinoline derivatives according to Scheme 2. The obtained compounds of **2O**, **2S**, and **2Se** showed yellow-green, yellow, and orange color, respectively, analogous to the model compounds. All three compounds were stable under air and soluble

Scheme 2. Synthesis of Monomers 2O, 2S, and 2Se

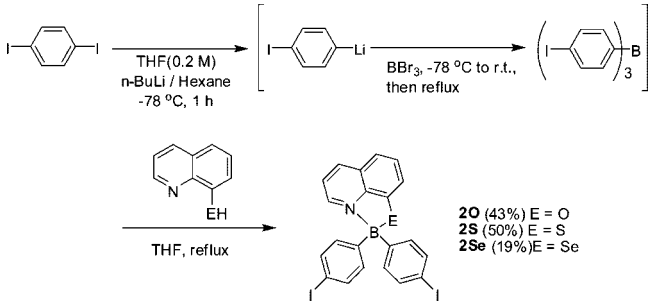

Table 2. Polymerization of Organoboron Quinolate-Based Monomers and 1,4-Diethynylbenzene Derivatives[a]

polymers	yield[b] (%)	M_n[c]	M_w[c]	M_w/M_n[c]	DP_n[d]	T_5/°C[e]	T_{10}/°C[e]
4OO	29	3200	6100	1.9	3.5	286	305
4OF	58	3400	4900	1.4	6.0	332	363
4SO	83	11200	24500	2.2	12.0	293	317
4SF	58	3100	5500	1.8	5.3	276	312
4SeO	87	7800	10900	1.4	8.0	293	318
4SeF	69	2200	6600	3.0	3.5	292	322

[a] Conditions: Sonogashira−Hagihara couplings of organoboron quinolate-based monomer (1 equiv) and 1,4-diethynylbenzene derivatives (1 equiv) were carried out in the presence of $Pd(PPh_3)_4$, CuI in the mixed solvent ($THF/NEt_3 = 2/1$) at room temperature or 40 °C for 96 or 48 h. [b] Isolated yields after precipitation. [c] Estimated by size-exclusion chromatography (SEC) based on polystyrene standard in tetrahydrofuran (THF). [d] Average number of repeating units calculated from M_n and molecular weights of repeating units [e] Thermogravimetric analysis: heating rate 10 K/min under air; values given for weight loss of 5% and 10%.

Table 3. UV−Visible Absorption and Photoluminescence Data

compounds	$\lambda_{abs,max}$ (nm)[a]	ε(m^2 mol^{-1})[a]	$\lambda_{em,max}$ (nm)[b]	Φ_F[b,c]
4OO	313, 374	3250, 3700	421, 502	0.54
4OF	264, 356, 372	2910, 5600, 5580	414, 501	0.58
4SO	287, 316, 374	2390, 2950, 3390	433, 564	0.10
4SF	279, 359, 375	1920, 3760, 3810	420, 561	0.14
4SeO	297, 314, 377	2820, 2920, 3450	427, 598	0.01
4SeF	287, 360, 377	1820, 3630, 3680	415, 601	0.00
1O	264, 395	2370, 220	501	0.47
1S	273, 454	1500, 260	563	0.09
1Se	283, 480	1440, 260	609[d]	0.01

[a] UV−vis: $CHCl_3$ (1.0×10^{-5} M). [b] Fluorescence: $CHCl_3$ (1.0×10^{-5} M). [c] Absolute quantum yield. [d] 1.0×10^{-3} M.

in dichloromethane and chloroform, whereas insoluble in hexane. The tetracoordination state of the boron atoms in **2S** and **2Se** were confirmed by the ^{11}B NMR spectroscopy in $CDCl_3$ [**2S**, δ_B = 7.43 ppm; **2Se**, δ_B = 7.53 ppm]. Because of electronegative property of iodine atom, these signals are downfield-shifted compared to those of the model compounds. Furthermore, the structures of **2S** and **2Se** were also characterized by ^1H NMR, ^{13}C NMR and electron-spray-ionization mass spectroscopies, and by elemental analysis.

Synthesis of Polymers. Scheme 3 and Table 1 summarize the condition and results of the polymerization of **2O**, **2S**, or **2Se** with 1,4-diethynylbenzene derivatives **3O** or **3F** in the presence of a catalytic amount of $Pd(PPh_3)_4$ and CuI in the mixed solvents of tetrahydrofuran (THF) and triethylamine. The polymers **4OO**, **4OF**, **4SO**, **4SF**, **4SeO**, and **4SeF** were obtained as yellow or orange solids after precipitation into methanol and hexane, respectively, and the polymer yields were 29−87%. The polymers were soluble in THF, CH_2Cl_2, and $CHCl_3$. The ^{11}B NMR spectra of the obtained polymers were observed at δ_B = 8.89−3.91 ppm assignable to the tetracoordination state of the boron atoms in each polymers, indicating that the polymerization proceeded without any damage to the structure in the organoboron quinolate moiety. The IR spectra of the polymers showed the absorption peaks at 2214−2204 cm^{-1}, which are attributable to stretching of the −C≡C− bond

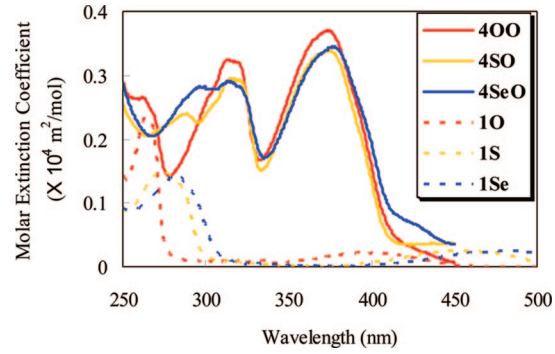

Figure 2. UV−vis spectra of polymers and model compounds in $CHCl_3$ (1.0×10^{-5} M).

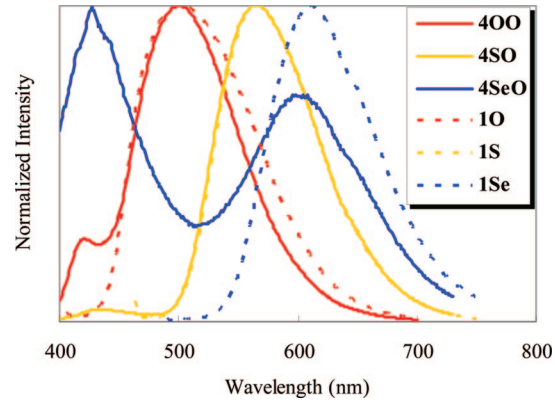

Figure 3. Normalized emission spectra of polymers and model compounds in $CHCl_3$ (1.0×10^{-5} M).

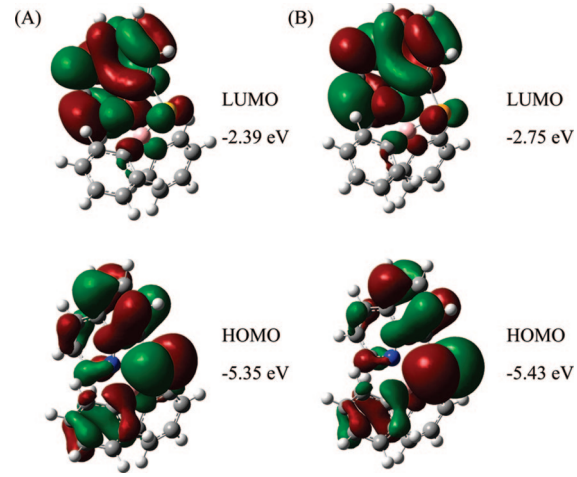

Figure 4. Molecular orbital diagrams for the HOMO and LUMO of (A) **1S** (B3LYP/6-31G(d)//B3LYP/6-31G(d)) and (B) **1Se** (B3LYP/6-311_+G(2df, 2p)//B3LYP/6-311+G(2df, 2p)).

in the polymer backbone. Moreover, strong peaks due to the C−F stretching band were observed at around 1157 cm^{-1} in the spectra of **4OF**, **4SF**, and **4SeF**. The number-average molecular weights (M_n) and the molecular weight distribution (M_w/M_n) of the polymers, measured by size-exclusion chromatography (SEC) in THF toward polystyrene standards, were 2200−11200 and 1.4−3.0, respectively (Table 2). Thermal stabilities of the polymers were examined by thermogravimetric analysis. The start of the thermal degradation under air for the polymers lies between 276 and 332 °C, where 5% weight loss was recorded. These data suggest that the obtained polymers present similar thermal stability to general poly(*p*-phenylene−ethynylene)s.[23]

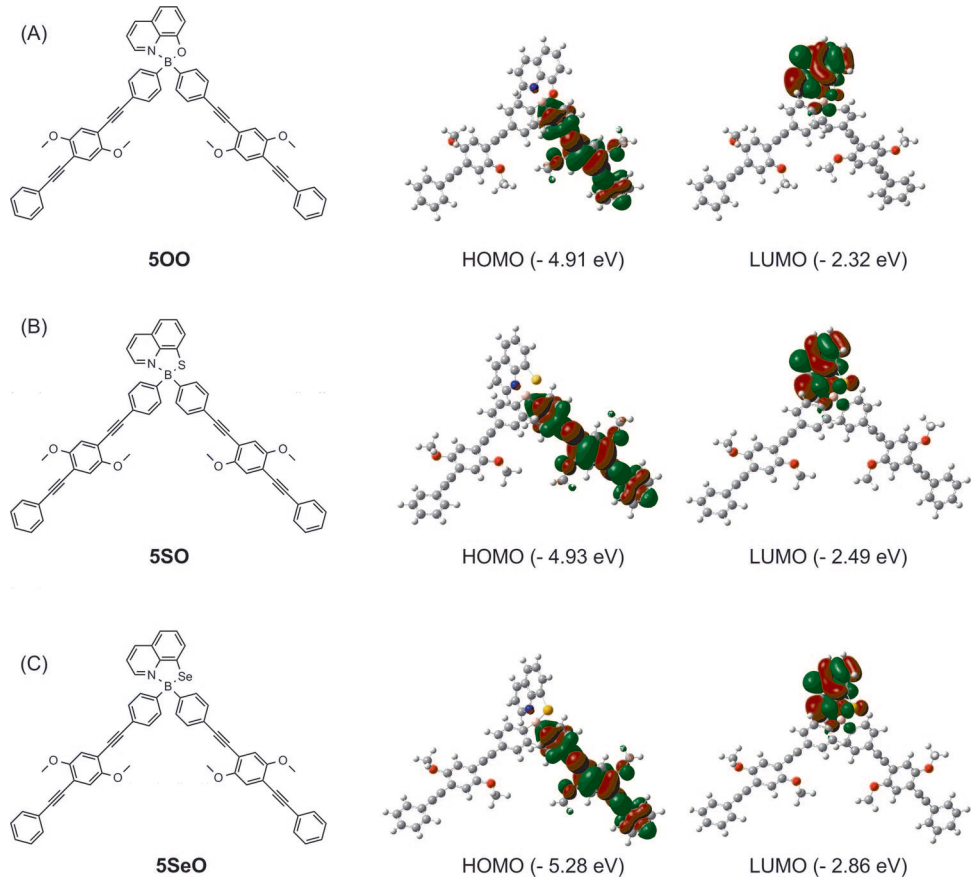

Figure 5. Structures and molecular orbital diagrams for the HOMO and LUMO of (A) **5OO** (B3LYP/6-31G(d)//B3LYP/6-31G(d)), (B) **5SO** (B3LYP/6-31G(d)//B3LYP/6-31G(d)), and (C) **5SeO** (B3LYP/6-311+G(2df, 2p)//B3LYP/6-31G(d)).

Scheme 3. Synthesis of Polymers

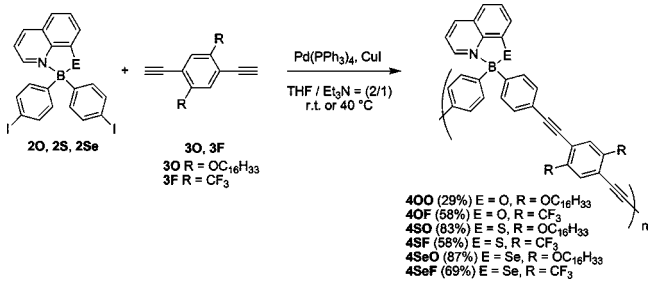

Optical Properties. The optical properties of the obtained polymers were investigated by UV−vis absorption and photoluminescence in $CHCl_3$ solution as compared to those of model compounds. The results from the absorption and emission spectra are summarized in Table 3. All emission data given here were obtained after exciting at the longest wavelength of the absorption peaks, i.e., absorption maxima of the polymers and the model compounds are corresponding to phenylene-ethynylene and quinoline, respectively. The model compounds **1O**, **1S**, and **1Se** showed the weak absorption peaks at 395 nm, 454 nm, and 480 nm, respectively, arising from the quinolinol ligand and the strong absorption peaks at around 270 nm, derived from the $\pi-\pi^*$ transition (Figure 2). The absorption peaks of the quinolinol ligand shift to longer wavelength as the covalent nature of the boron−ligand bonding is increased, that is, the maximum of **1Se** is red-shifted as compared to that of **1S** which, in turn, is red-shifted in comparison with that of **1O**. Despite the absorption peaks of the model compounds, this observation seems to confirm the expected trend from the rule, as mentioned above, which govern the absorption and fluorescence of metal chelates of Q. In contrast to the model compounds, the polymers **4OO**, **4OF**, **4SO**, **4SF**, **4SeO**, and **4SeF** showed the strong absorption peaks in the region from 300 to 400 nm. These peaks should be due to the π-conjugated linkers connecting the Q units each other. It is observed that the polymers which have the same π-conjugated linkers give the same absorption peaks in the region from 300 to 400 nm. This would mean that the electronic structure of the π-conjugated linker is independent from that of the Q ligand.

In the photoluminescence spectra in $CHCl_3$, model compounds **1O**, **1S**, and **1Se** showed emission maxima at 501 nm, 563 nm, and 609 nm, respectively (Figure 3). The emission shifts to longer wavelength as the covalent nature of the boron-ligand bonding is increased. The absolute fluorescence quantum yields of **1O**, **1S**, and **1Se** in $CHCl_3$ at room temperature were determined as $\Phi_F = 0.47$, 0.09, and 0.01, respectively. Fluorescence is reduced with increasing atomic number of the 16 Group atom that is adjacent to the boron atom in each model compound, caused by an increase in the rate of intersystem crossing known as heavy atom effect. From these results, it can be said that the model compounds emit from the Q-based ILCT excited-state and follow the rules similar to those govern the fluorescence of metal chelates of Q. The photoluminescence spectra of polymers **4OO**, **4SO**, and **4SeO** are also represented in Figure 3. Noteworthily, the shapes of the emission spectra of the polymers **4OO** and **4SO** are quite analogous to the corresponding model compounds. Therefore the photoluminescence spectra of these polymers are characteristic of the Q ligands. In other words, the presence of organoboron quinolate in the polymer backbone is crucial in these photoluminescence properties. It can be deduced that the energy transfer from the π-conjugated linkers in the main-chain to the Q ligands on the boron centers would occur not only in **4OO**, but also in **4SO**. On the other hand, **4SeO** showed the strong peak at 427

nm, emitting from π-conjugated linker and the weak peak at 598 nm, emitting from Q ligand in the photoluminescence spectrum. There are no differences between the polymers with the donating π-conjugated linker and with the accepting one in the photoluminescence property, as shown in Table 3. This means that the π-conjugated linker is irresponsible to both the emission spectrum and absolute quantum yield. In comparison with quantum yields, it can be seen that absolute quantum yields of the polymers are nearly equal to the corresponding model compounds, thereby implying the efficient energy transfer from the π-conjugated linkers to the Q ligands. Furthermore, the polymers **4SO** and **4SeO** have high refractive indices, $n_d = 1.67$ and 1.68, respectively. These values were high enough in comparison with those of S-containing polymers such as polythiourethane known as high refractive materials, indicating the potential applicability to optical devices.[24]

Molecular Orbital Calculations. To further understand the nature of optical properties, we have carried out theoretical calculation for compounds **1S**, **1Se**, **5OO**, **5SO**, and **5SeO** using density-functional theory (DFT) method at the B3LYP/6-31G(d) or B3LYP/6-311$_+$G(2df, 2p).[25] Parts A and B of Figure 4 exhibit LUMO and HOMO of **1S** and **1Se**, respectively. The LUMOs of these compounds are located predominantly on Q ligands and the HOMOs are on Q ligands and phenyl group. As a result, the HOMO−LUMO transition is not restricted but the molar extinction coefficient is low. In addition, the HOMO and LUMO of these compounds are partly located on S or Se atoms, which leads to a smaller HOMO−LUMO gap for **1Se** (2.68 eV) relative to **1S** (2.96 eV). In contrast, the HOMOs of compounds **5OO**, **5SO**, and **5SeO**, which have π-conjugated linkers, are not on the Q ligands, but localized on the whole of π-conjugated linkers and the LUMOs are localized on the Q ligands, as shown in Figure 5. These spatial separations of HOMOs and LUMOs probably decrease the electronic transition dipoles and the oscillator strengths of HOMO−LUMO transitions of the polymers. In fact, TD-DFT calculations of **1S** and **5SO** support this explanation. The calculated oscillator strengths *f*s of HOMO−LUMO transitions were 0.0593 for **1S** and 0.0067 for **5SO**. From these results, it can be said that the HOMO−LUMO transitions are not allowed but the $\pi-\pi^*$ transitions of π-conjugated linkers contribute to the absorption peak of lowest energy in the UV−vis absorption spectrum. Moreover, the HOMOs of **5OO**, **5SO**, and **5SeO** are not located on the 16 group atoms that are adjacent to the boron atom in each polymer, indicating that the $\pi-\pi^*$ transitions of π-conjugated linkers are not responsible to these atoms.

Conclusion

In conclusion, we have prepared the novel low-molecular-mass organoboron quinoline-8-thiolate and -selenolate complexes (model compounds) and the main-chain-type organoboron quinoline-8-thiolate and -selenolate polymers. These polymers were obtained by Sonogashira−Hagihara coupling in moderate yields. The emission shifted to longer wavelength as the covalent nature of the boron-ligand bonding is increased and the absolute quantum yield was reduced with increasing atomic number of the 16 group atom adjacent to the boron atom. Emission behavior of the polymers originated efficient energy transfer from π-conjugated main chain to Q ligand and showed no difference in emission between the donating π-conjugated linker and accepting one. In addition, the polymers had high refractive indices, so that further study of these polymers may lead to a new class of materials with both luminescence and high refractive index.

Supporting Information Available: Cif files for **1S** and **1Se** containing crystallographic data. This material is available free of charge via the Internet at http://pubs.acs.org.

References and Notes

(1) (a) Hadziioannou, G., van Hutten, P. F., Eds., *Semiconducting polymers: Chemistry, Physics and Engineering*, 2nd ed.; Wiley-VCH: Weinheim, Germany, 2006. (b) Skotheim, T. J., Elsenbaumer, R. L. Reynolds, J. R., Eds. *Handbook of Conducting Polymers*, 2nd ed.; Dekker: New York, 1998. (c) Martin, R. E.; Diederich, F. *Angew. Chem.* **1999**, *111*, 1440.

(2) Kraft, A.; Grimsdale, A. C.; Holmes, A. B. *Angew. Chem.* **1998**, *110*, 416.

(3) Hide, F.; Diaz-Garcia, M. A.; Schwartz, B. J.; Heeger, A. J. *Acc. Chem. Res.* **1997**, *30*, 430.

(4) Screen, T. E. O.; Lawton, K. B.; Wilson, G. S.; Dolney, N.; Ispasoiu, R.; Goodson, T., III; Martin, S. J.; Bradley, D. D. C.; Anderson, H. L. *J. Mater. Chem* **2001**, *11*, 312.

(5) Yu, G.; Gao, J.; Hummelen, J. C.; Wudl, F.; Heeger, A. J. *Science* **1995**, *270*, 1789.

(6) (a) Bao, Z.; Rogers, J. A.; Katz, H. E. *J. Mater. Chem.* **1999**, *9*, 1895. (b) Calvert, P. *Chem. Mater.* **2001**, *13*, 3299.

(7) Haugland, R. P. In *The Handbook-A Guide to Fluorescent Probes and Labeling Technologies*, 10th ed.; Spence, M. T. Z., Ed.; Molecular Probes: Eugene. OR, 2005; Chapter 1, Section 1.4.

(8) Gorman, A.; Killoran, J.; O'Shea, C.; Kenna, T.; Gallagher, W. M.; O'Shea, D. F. *J. Am. Chem. Soc.* **2004**, *126*, 10619.

(9) (a) García-Moreno, I.; Costela, A.; Campo, L.; Sastre, R.; Amat-Guerri, F.; Liras, M.; López Arbeloa, I. *J. Phys. Chem. A* **2004**, *108*, 3315. (b) Pavlopoulos, T. G.; Boyer, J. H.; Sathyamoorthi, G. *Appl. Opt.* **1998**, *37*, 7797.

(10) (a) Nagata, Y.; Chujo, Y. *Macromolecules* **2007**, *40*, 6. (b) Nagata, Y.; Chujo, Y. *Macromolecules* **2008**, *41*, 2809.

(11) (a) Cheng, Y. M.; Yeh, Y. S.; Ho, M. L.; Chou, P. T.; Chen, P. S.; Chi, Y. *Inorg. Chem.* **2005**, *44*, 4594. (b) Shi, Y.-W.; Shi, M.-M.; Huang, J.-C.; Chen, H.-Z.; Wang, M.; Liu, X.-D.; Ma, Y.-G.; Xu, H.; Yang, B. *Chem. Commun.* **2006**, 1941.

(12) (a) Chen, C. H.; Shi, J. C. *Coord. Chem. Rev.* **1998**, *171*, 161. (b) Ballardini, R.; Varani, G.; Indelli, M. T.; Scandola, F. *Inorg. Chem.* **1986**, *25*, 3858.

(13) Shavaleev, N. M.; Adams, H.; Best, J.; Edge, R.; Navaratnam, S.; Weinstein, J. A. *Inorg. Chem.* **2006**, *45*, 9410.

(14) Higashi, T. *ABSCOR. Program for Absorption Correction*; Rigaku Corporation: Tokyo, Japan, 1995.

(15) Sheldrick, G. M. *SHELX-97. Programs for Crystal Structure Analysis.*; University of Göttingen: Göttingen, Germany, 1997.

(16) Altomare, A.; Burla, M. C.; Camalli, M.; Cascarano, G. L.; Giacovazzo, C.; Guagliardi, A.; Moliterni, A. G. G.; Polidori, G.; Spagna, R. *J. Appl. Crystallogr.* **1999**, *32*, 115.

(17) Wakita, K. *Yadokari-XG. Program for Crystal Structure Analysis*; **2000**.

(18) Farrugia, L. J. *J. Appl. Crystallogr.* **1997**, *30*, 565.

(19) Ashaks, J.; Bankovsky, Y.; Zaruma, D.; Shestakova, I.; Domracheva, I.; Nesterova, A.; Lukevics, E. *Chem. Heterocycl. Compd.* **2004**, *40*, 776.

(20) Swager, T. M.; Gil, C. J.; Wrighton, M. S. *J. Phys. Chem.* **1995**, *99*, 4886.

(21) Nagai, A.; Miyake, J.; Kokado, K.; Nagata, Y.; Chujo, Y. *J. Am. Chem. Soc.* **2008**, *130*, 15276.

(22) Wu, Q.; Esteghamatian, M.; Hu, N.-X.; Popovic, Z.; Enright, G.; Tao, Y.; D'Iorio, M.; Wang, S. *Chem. Mater.* **2000**, *12*, 79.

(23) Egbe, D. A. M.; Roll, C. P.; Brickner, E.; Grummt, U.-W.; Stockmann, R.; Klemm, E. *Macromolecules* **2002**, *35*, 3825.

(24) Okubo, T.; Kohmoto, S.; Yamamoto, M. *J. Polym. Sci., Part A: Polym. Chem.* **1998**, *68*, 1791.

(25) Frisch, M. J.; Trucks, G. W.; Schlegel, H. B.; Scuseria, G. E.; Robb, M. A.; Cheeseman, J. R.; Montgomery, J. A., Jr.; Vreven, T.; Kudin, K. N.; Burant, J. C.; Millam, J. M.; Iyengar, S. S.; Tomasi, J.; Barone, V.; Mennucci, B.; Cossi, M.; Scalmani, G.; Rega, N.; Petersson, G. A.; Nakatsuji, H.; Hada, M.; Ehara, M.; Toyota, K.; Fukuda, R.; Hasegawa, J.; Ishida, M.; Nakajima, T.; Honda, Y.; Kitao, O.; Nakai, H.; Klene, M.; Li, X.; Knox, J. E.; Hratchian, H. P.; Cross, J. B.; Adamo, C.; Jaramillo, J.; Gomperts, R.; Stratmann, R. E.; Yazyev, O.; Austin, A. J.; Cammi, R.; Pomelli, C.; Ochterski, J. W.; Ayala, P. Y.; Morokuma, K.; Voth, G. A.; Salvador, P.; Dannenberg, J. J.; Zakrzewski, V. G.; Dapprich, S.; Daniels, A. D.; Strain, M. C.; Farkas, O.; Malick, D. K.; Rabuck, A. D.; Raghavachari, K.; Foresman, J. B.; Ortiz, J. V.; Cui, Q.; Baboul, A. G.; Clifford, S.; Cioslowski, J.; Stefanov, B. B.; Liu, G.; Liashenko, A.; Piskorz, P.; Komaromi, I.; Martin, R. L.; Fox, D. J.; Keith, T.; Al-Laham, M. A.; Peng, C. Y.; Nanayakkara, A.; Challacombe, M.; Gill, P. M. W.; Johnson, B.; Chen, W.; Wong, M. W.; Gonzalez, C.; Pople, J. A. *Gaussian 03, revision D.01*; Gaussian, Inc.: Wallingford, CT, 2004.

MA900008M